The effect of highly alkaline water (pH 9.5) on the morphology and morphometry of chloride cells and pavement cells in the gills of the freshwater rainbow trout: relationship to ionic transport and ammonia excretion

Pierre Laurent, Michael P. Wilkie, Claudine Chevalier, and Chris M. Wood

Abstract: Exposure of rainbow trout (*Oncorhynchus mykiss*) to alkaline water (pH 9.5) impairs ammonia excretion (J_{Amm}) and gill-mediated ion-exchange processes, as characterized by decreased Cl^- (J_{in}^{Cl}) and Na^+ influx (J_{in}^{Na}) across the gill. Scanning electron microscopy suggested that the depression of J_{in}^{Cl} was concomitant with an early decrease in the population of the most active chloride cells (CCs), partly compensated for by an increasing number of immature CCs. However, within 72 h after the onset of exposure to alkaline water, there was a 2-fold increase in the fractional apical surface area of CCs that paralleled complete recovery of the maximal Cl^- influx rate (J_{max}^{Cl}). These results suggest that recovery of J_{max}^{Cl} was associated with greater CC surface area, resulting in more transport sites on the gill epithelium. Morphometric analysis of the outermost layer of pavement cells on the lamellar epithelium showed a greater density of microvilli during exposure to alkaline water, which may have contributed to partial restoration of the number of Na^+ transport sites (J_{max}^{Na}). Finally, the blood-to-water gill-diffusion distance decreased by 27% after 72 h at pH 9.5, and likely contributed to progressive restoration of ammonia excretion in alkaline water.

Résumé : L'exposition de la Truite arc-en-ciel (*Oncorhynchus mykiss*) à de l'eau alcaline (pH 9,5) cause d'importantes modifications morphologiques dans l'epithélium branchial. Ces modifications visent à contrebalancer des troubles fonctionnels comme l'inhibition de l'excretion d'ammoniaque (J_{Amm}) et la diminution des flux entrants de Cl^- (J_{in}^{Cl}) et de Na^+(J_{in}^{Na}) à travers la branchie. La microscopie électronique à balayage a montré que la diminution de J_{in}^{Cl} était concomitante d'une diminution rapide de la population des cellules à chlorure les plus actives partiellement compensée par une augmentation des cellules à chlorure immatures. Cependant dans les 72 h qui suivent le début de l'exposition alcaline, on a observé un dédoublement de la surface fractionnelle apicale des cellules à chlorure en parallèle avec la restauration complète du flux entrant maximal de Cl^- (J_{max}^{Cl}). Ces résultats suggèrent que le rétablissement de J_{max}^{Cl} est associé à une plus grande surface de cellules à chlorure et donc à un plus grand nombre de sites de transport par unité de surface épithéliale branchiale. L'analyse morphométrique de la surface apicale des cellules pavimenteuses a montré une augmentation de la densité des microvillosités pendant une exposition alcaline, contribuant ainsi à la restauration partielle du nombre des sites de transport de Na^+ (J_{max}^{Na}). Finalement, la distance de diffusion eau-sang a diminué de 27 %, contribuant ainsi à la restauration progressive de l'excrétion d'ammoniaque en milieu alcalin.

Introduction

Although the rainbow trout (*Oncorhynchus mykiss*) does not normally live in alkaline (pH ≥ 9.4) waters, some individuals may be subjected to temporary upward pH surges due to the photosynthetic processes of macrophytes and algae (Halstead and Tash 1982; Murray and Zeibell 1984), anthropogenic factors (Heming and Blumhagen 1988), or stocking into naturally alkaline lakes (Kucera et al. 1985; Coleman and Johnson 1988; Wagner et al. 1997). Indeed, attempts to stock salmonids into many alkaline saline lakes have been complicated by the inability of the fish to adjust readily to high pH (Coleman and Johnson 1988; Wagner et al. 1997). One major problem often encountered by salmonids in alkaline environments is a severe depression of plasma electrolyte levels, which may be lethal if not corrected (Yesaki and Iwama 1992; Wilkie et al. 1993). Our recent results using rainbow trout demonstrated that this depression

Received January 19, 1999. Accepted September 23, 1999.

Pierre Laurent. Centre National de la Recherche Scientifique, Centre d'Ecologie et de Physiologie Energétiques, Laboratoire de Morphologie Fonctionnelle et Ultrastructurale des Adaptations, Strasbourg, France, F-67037, and Department of Biology, McMaster University, Hamilton, ON L8S 4K1, Canada.
Michael P. Wilkie[1] and Chris M. Wood. Department of Biology, McMaster University, Hamilton, ON L8S 4K1, Canada.
Claudine Chevalier. Centre National de la Recherche Scientifique, Centre d'Ecologie et de Physiologie Energétiques, Laboratoire de Morphologie Fonctionnelle et Ultrastructurale des Adaptations, Strasbourg, France, F-67037.

[1]Author to whom all correspondence should be sent at the following address: Division of Life Sciences, University of Toronto at Scarborough, 1265 Military Trial, Scarborough, ON M1C 1A4, Canada (e-mail: wilkie@scar.utoronto.ca).

of plasma chloride (Cl^-) and sodium (Na^+) levels was due to initial 60–70% reductions in Cl^- influx (J_{in}^{Cl}) and Na^+ influx (J_{in}^{Na}; Wilkie et al. 1999), but that alkaline water (pH 9.5) affected outflux (diffusive ion loss) only slightly. The reductions in Cl^- influx were due to a transient 50% reduction in the maximal Cl^- uptake rate (J_{max}^{Cl}), but Cl^- influx recovered after 3 d of exposure to an alkaline environment (Wilkie et al. 1999). Since chloride cells (CCs) are the probable site of Cl^- uptake across the fish gill (reviewed by Laurent and Perry 1995; Goss et al. 1995; Perry 1997), one goal of the present study was to relate changes in CC morphology to Cl^- influx patterns during alkaline exposure.

Alkaline water also reduced the maximal Na^+ uptake rate (J_{max}^{Na}) by 70%, but this was partially restored after 72 h. The affinity of the gill for Na^+ transport was reduced at this time, however, as reflected by a 4-fold increase in K_m^{Na} (Wilkie et al. 1999). Although J_{in}^{Na} was chronically reduced in trout at high pH, net Na^+ balance was eventually restored, owing to a progressive counterbalancing reduction in Na^+ outflux (J_{out}^{Na}). In view of these results, a second goal of the present study was to relate possible changes in transbranchial Na^+ movements to alterations in gill architecture at pH 9.5. Pavement cell (PVC) morphology was a particular focus in this regard, in view of the recent finding that these cells may be important in Na^+ uptake (Goss et al. 1992, 1994*a*, 1995; Laurent et al. 1994; Sullivan et al. 1995).

Although ammonia excretion (J_{Amm}) is initially inhibited at high pH, it generally recovers after 1–3 d, owing to the retention of ammonia, which leads to a progressive rise in the blood–water P_{NH_3} diffusion gradient (Wright and Wood 1985; Wilkie and Wood 1991, 1995; Yesaki and Iwama 1992; Wright 1993; Wilkie et al. 1999). In the present study these findings have been confirmed, but Laurent and Hebibi (1989) suggested that adjusting the length of the diffusion pathway is one mechanism that could also be used to modulate J_{Amm}. Thus, a final objective of the present investigation was to relate the changes in ammonia-excretion patterns at high pH to possible reductions of the blood-to-water diffusion distance across the gill.

Materials and methods

Rainbow trout (175–250 g) of both sexes were obtained from Spring Valley Trout Farm, Petersburg, Ontario, and acclimated to hard dechlorinated Hamilton tap water (composition ($mmol \cdot L^{-1}$): $[Na^+] = 0.6$; $[Cl^-] = 0.8$; $[Ca^{2+}] = 0.9$; $[Mg^{2+}] = 0.4$; titratable alkalinity = 2.0) at 13–15°C. Complete details of holding conditions and the experimental set-up are given by Wilkie et al. (1999). Briefly, 1 week before experiments, fish were transferred in batches of 10 to an isolation tank set to the experimental temperature of 13–15°C. Food was withheld at this time to minimize the known effects of feeding on nitrogenous-waste metabolism in fish (Brett and Zala 1975). Two days before experiments, rainbow trout were removed from their isolation tank and quickly transferred to darkened individual Plexiglas flux boxes of about 2.0 L volume. The chambers were well aerated to ensure that water was sufficiently oxygenated and mixed when water flow to the boxes was terminated during determinations of maximal Cl^- and Na^+ influx rates (J_{max}^{Cl}, J_{max}^{Na}), along with ammonia-excretion rates (J_{Amm}). The chambers were part of a flow-through system consisting of a pH stat set-up that kept the water entering the flux chambers at a nominal pH of 9.5 through the addition of 1 $mol \cdot L^{-1}$ KOH to the system's head-tank reservoir (for complete details see Wilkie et al. 1999).

Experimental protocol

After the 2-d acclimation period in the flux chambers, the trout were either left at pH 8.0 (controls) or subjected to pH 9.5 for 10, 24, or 72 h. Ion uptake kinetics experiments and determinations of ammonia-excretion rate were performed on 6–8 fish under control conditions or at high pH. To determine J_{max}^{Cl} and J_{max}^{Na}, the influx rates for each ion were made at sequentially higher concentrations of NaCl in the water, using ^{36}Cl and ^{22}Na. Influx rates were based on the measured change in the water mean specific activity of each isotope and the respective changes in total water Cl^- or Na^+ concentrations during each 30- to 60-min flux period (cf. Wilkie et al. 1999). The ammonia concentrations of water samples were also determined, which enabled us to determine the ammonia-excretion rate for each fish as described by Wilkie and Wood (1994).

Following completion of the ion uptake kinetics experiments, the trout held at pH 8.0 or exposed to pH 9.5 were sacrificed with an overdose of neutralized MS 222 ($1.5\ g \cdot L^{-1}$). Other than exposure to pH 9.5, the control trout held at pH 8.0 were treated identically with the experimental animals. Although the periods of enclosure in the flux boxes were not identical for all groups of animals, our previous studies indicated that this variable has no effect on either plasma cortisol level (Wilkie et al. 1996) or gill ultrastructure (Wilkie and Wood 1994).

Immediately following death, the gill arches (right side) were excised from each trout and quickly rinsed in ice-cold sodium cacodylate ($0.15\ mol \cdot L^{-1}$). The individual gill filaments were then carefully dissected away from each gill arch in the buffer, then fixed for transmission electron microscopy (TEM) or scanning electron microscopy (SEM) as outlined by Laurent and Perry (1990) and Goss et al. (1992). The completely fixed gills were then used for the morphometric studies described below. This approach enabled us to directly compare gill morphometric data for each period with the respective ion-uptake kinetics reported for the groups of fish described by Wilkie et al. (1999).

Preparation of samples and measurements

Each piece of gill arch contained several pairs of filaments (anterior and posterior rows), from which most of the arch tissue was removed. Only the anterior and posterior rows of filaments remained attached to the septum of the arch. The gill samples were subsequently processed for SEM and TEM according to methods described in detail elsewhere (Laurent 1984; Laurent and Hebibi 1989; Perry and Laurent 1989). In addition to qualitative studies of gill ultrastructure, morphometric measurements were also performed using scanning electron and transmission electron micrographs.

SEM morphometry entailed measuring individual apical surface areas and numerical density of chloride cells (CCs) to allow calculation of their fractional apical surface area (i.e., the relative area occupied by the parts of CCs exposed to the external medium) according to methods described previously (Laurent and Hebibi 1989; Laurent and Perry 1990). Measurement of the density of microvilli permitted individual CCs to be divided into three categories according to the nature of their apical surfaces: (1) smooth (no villi); (2) moderately villous (up to 8 microvilli$\cdot \mu m^{-2}$); and (3) highly villous (more than 8 microvilli$\cdot \mu m^{-2}$). Dead or dying CCs have a smooth apical surface, but to determine if the cells were apoptotic or necrotic, it was necessary to analyze the intracellular morphology of the cell using TEM (see below). For SEM morphometry, at least 10 noncontiguous fields of the filamental epithelium close to the base of the lamellae were photographed on each fish. Statistical methods have been described previously (Laurent and Hebibi 1989; Laurent and Perry 1990).

TEM morphometry of CCs and intracellular organelles was carried out on photographs (magnification 10 000 ×) of ultrathin cross sections of epithelium from 5 filaments from the first gill arch (a total of 25 photographs from each fish). This morphometry entailed dividing CCs into three categories: (1) immature and mature; (2) apoptotic; and (3) necrotic. The criteria used for this procedure are described and interpreted in the Discussion. The percentage of CCs in each category was calculated for each group of fish. Volume density as a percentage of cell volume, and the surface area : volume ratio of CC mitochondria and cell tubules, were estimated morphometrically. Assessment of these parameters was necessary for identifying the degree of functionality of CCs. These measurements were done according to Weibel et al. (1966) in which an overlaid square lattice of parallel short segments that intersects the surface of the structure in question is used and the ends of the lattice segments are counted according to their location inside the structure.

The blood-to-water diffusion distance was calculated by randomly superimposing a circular grid on transmission electron micrographs. This grid consisted of the ends of short sampling lines oriented in three directions (for details see Weibel and Knight 1964; Laurent and Hebibi 1989). Nine different grid positions were averaged on each photograph of a lamella cross section. Twenty cross sections from each fish were photographed and the data averaged for each fish.

Pavement cell surface morphology

PVCs constitute the outermost layer of the lamellar epithelium. Contrary to earlier opinion, there now exists a body of morphological and physiological evidence that PVCs participate in ion exchange (see the Introduction). The apical surface area of PVCs can be estimated morphometrically using a surface density test. Unlike subcellular structures (mitochondria, tubules), which are more or less isotropic (i.e., oriented in no particular direction), the apical plasma membrane of the PVC is anisotropic. In the present case, as suggested by Weibel and Bolender (1973), the curvilinear test system grid of Merz (1968) was superimposed on 20 different TEM lamellar profiles per fish, photographed at a final magnification of 8640×. This provided a reference counting area of 100 μm^2. The intersections were then counted, and the number, P_T, was used to calculate the actual surface area of section A_T, which is described by

$$A_T = P_T \cdot d^2$$

where d corresponds to the diameter of the semicircles corrected by the magnification (8640×).

Statistics

Data are expressed as the mean ± 1 SEM, followed by the number of fish (N) in parentheses, except in Fig. 4, where N is the number of CCs analyzed for the frequency distribution of different CC types. The significance of differences between frequency distributions was analyzed by the χ^2 test, and differences between means were evaluated using the nonparametric Kruskal–Wallis test or one-way ANOVA followed by Dunn's or the Bonferroni post-test method ($P < 0.05$) as appropriate.

Results

The mean values of individual apical surface areas, numerical densities, and fractional areas of the total CC population (the sum of smooth, moderately villous, and highly villous CCs; see below) were obtained from SEM photos (e.g., Fig. 6) and are presented in Fig. 1. All three parameters increased significantly after 72 h in alkaline conditions (pH 9.5), with a nonsignificant upward trend in density and surface area at 10 h. By 72 h, numerical density rose by 77% (Fig. 1B) and individual apical surface area increased by 42% (Fig. 1C), leading to an overall increase in fractional apical surface area of 128% (Fig. 1A).

In general, previous morphofunctional assessments of CCs have suggested that the density of microvilli in CCs reflects the cells' functional status (Laurent and Perry 1990; Wendelaar Bonga and van der Meij 1989). Accordingly, in the present study, CCs were categorized as highly villous, moderately villous, or smooth (no microvilli; Figs. 1, 6). In the context of the present study, highly villous and moderately villous CCs were considered functional, since in all likelihood they represent mature and young CCs, respectively. However, smooth cells likely represent swollen CCs that have lost their ability to regulate their volume and are therefore nonfunctional or "worn out" (compare Figs. 6A and 6B; Laurent and Perry 1990).

After 10 h at pH 9.5, there were significant reductions in the numerical density (Fig. 1B) and individual surface area (Fig. 1C) of highly villous CCs, leading to a marked (80%) decrease in the fractional surface area of highly villous CCs at this time (Fig. 1A). The fractional surface area of highly villous CCs was partially regained by 72 h, while the fractional surface area (Figs. 1A, 6) of both moderately villous and smooth CCs increased progressively throughout the alkaline exposure, owing to significant changes in both the density and surface area of the CCs (Figs. 1B, 1C, 6).

The volume densities and the surface area : volume ratios of the mitochondria and tubules, which are the most characteristic organelles present in functional and nonfunctional (apoptotic and necrotic) CCs, were also quantified (Fig. 2). The percentage of the total cell volume (nucleus not included) occupied by mitochondria, about 20%, was not significantly affected by exposure to high pH for either 10 or 72 h (Fig. 2A). In contrast, the volume density of intracytoplasmic tubules decreased dramatically within the first 10 h after exposure to pH 9.5, recovering to a value close to control levels by 72 h (Fig. 2A). Surface area : volume ratios (unit surface area per unit volume of the compartment) of tubules increased within the first 10 h after the onset of exposure to high pH and returned to control values by 72 h (Fig. 2B). These observations reflect the fact that at 10 h, the cellular volume occupied by these organelles contained numerous, but very narrow, tubules. The much lower surface area : volume ratio of the mitochondria did not change in response to exposure to high pH (Fig. 2B).

A total of 230 CCs from the entire population of fish studied (controls, and 10 and 72 h at pH 9.5) were sorted and placed in one of three categories, based on morphological criteria that likely relate to the functional status of CCs (see the Discussion): functional (immature and mature), apoptotic, or necrotic (Fig. 3). Mature cells have a characteristic appearance, which has been repeatedly described in the literature: a well-organized dense network of tubules (basolateral membrane invaginations) closely associated with a large number of mitochondria (Fig. 7B). Immature CCs display similar characteristics but have a less developed network of tubules according to the degree of differentiation (Fig. 7A). Since the differences between mature and immature CCs are not always clear, they are combined as "functional" in our

Fig. 1. Alterations in the fractional apical surface area (A), numerical density (B), and individual cell apical surface area (C) of chloride cells (CCs) on the filamental epithelium of rainbow trout gills at pH 8.0 (control) or after transfer to pH 9.5. CCs were also assigned to one of three classes according to the density of microvilli on their apical surface. Accordingly, the proportions of CCs having a smooth (no villi; solid bar), moderately villous (hatched bar), or highly villous (open bar) apical surface are also illustrated. Fractional apical surface areas of CCs are calculated from the data presented in B and C. Values are expressed as the mean ± 1 SEM (N = 6–7). An asterisk (*) indicates a statistically significant difference from control values for entire CC populations; a dagger (†), double dagger (‡), or star (☆) indicates a statistically significant difference from values at pH 8.0 for smooth, moderately villous, or highly villous CCs, respectively.

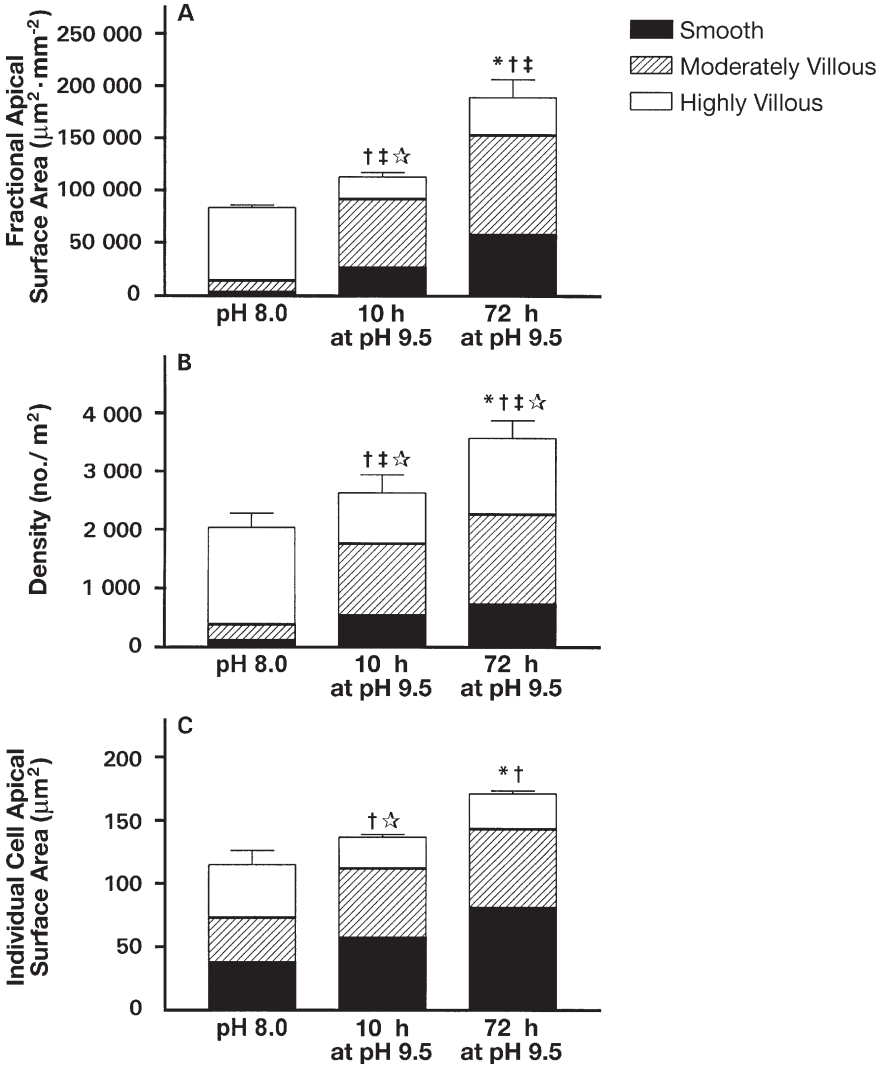

classification. The differences between nonfunctional apoptotic (Figs. 7A, 7C) and necrotic CCs (Fig. 8) are clear-cut and have been summarized by Wendelaar Bonga and van der Meij 1989; new information about the internal structure of the three CC categories is outlined below, based on analysis of the three cell types from all treatments.

Figure 3A demonstrates that mitochondrial volume density (in other words, the fractional volume occupied by mitochondria) was not significantly affected by the functional status of the CCs. In necrotic CCs, values were more variable because of mitochondrial alteration, but again there was no significant difference. An absence of differences was also seen in the mitochondrial surface area : volume ratio (Fig. 3B). In contrast, we observed large changes in the quantitative morphology of the tubules. Generally, tubules occupied about 12% of the cell volume (nucleus not included) in functional (immature or mature) CCs, but this value was more than 2-fold higher in apoptotic cells (Fig. 3A). Indeed, in functional CCs, tubules are quite narrow (smaller volume). The surface area : volume ratio (Fig. 3B), i.e, the membrane surface area per unit of tubular compartment volume, was greater in functional cells but significantly smaller in apoptotic cells. This is consistent with the high volume of the tubules in apoptotic cells (Fig. 3A).

A few hours after transfer to high pH, the percentage of functional CCs increased from 44 to 72%, whereas the percentage of apoptotic cells decreased from 55 to 23% (Fig. 4). By 72 h, however, the frequency distribution of the

Fig. 2. Changes in the morphometry of CC mitochondria (open bars) and tubules (hatched bars) in rainbow trout gills during exposure to pH 9.5 in terms of volume density as a percentage of total cell volume (A) and surface area : volume ratio (B). All data are expressed as the mean ± 1 SEM (N = 6–7 fish). An asterisk (*) indicates a statistically significant difference from values at pH 8.0 (control).

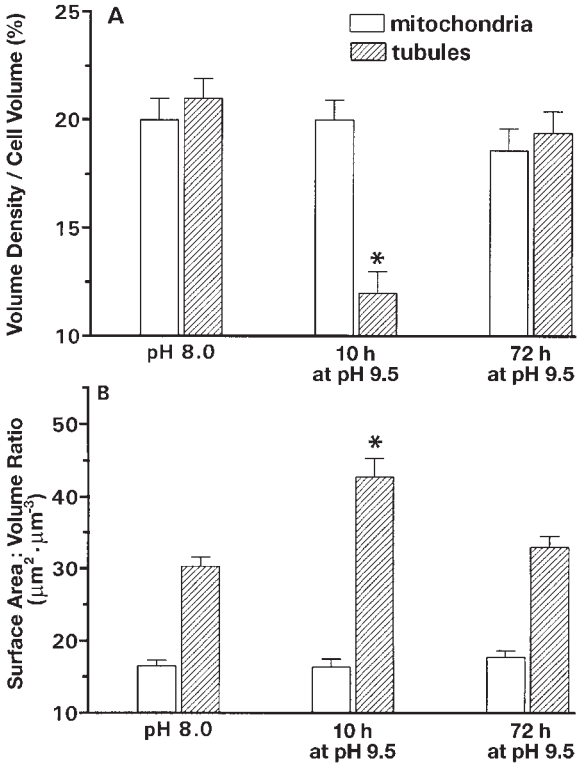

Table 1. Changes in ammonia excretion rates (J_{Amm}) and plasma total ammonia concentration (T_{Amm}) during exposure of rainbow trout to pH 9.5 for 72 h.

pH	Time (h)	J_{Amm} (μmol·kg^{-1}·h^{-1})	Plasma T_{Amm} (μmol·L^{-1})
8.0	C	135.7±12.7	84.7±13.8
9.5	3	28.7±3.3*	—
	10	64.6±8.6*	358.4±81.5*
	24	98.8±25.8	577.9±65.0*
	48	164.9±47.1	—
	72	165.0±29.8	285.0±59.4*

Note: Values are given as the mean ± 1 SEM (N = 6–7). "C" denotes control (pH 8.0) conditions.
*Significantly different from control values (P < 0.05).

three CC types had returned to a pattern not significantly different from control values (Fig. 4). The density of necrotic cells was not significantly altered at pH 9.5.

The length of the blood-to-water diffusion pathway was assessed from about 50 transmission electron micrographs per fish taken at each sampling time. By 10 h, there was a slight fall (nonsignificant) in the diffusion distance, which became more substantial (a 27% decrease) and highly significant by 72 h (Fig. 5A). These morphological changes were

Fig. 3. Differences in the morphometry of mitochondria (open bars) and tubules (hatched bars) in functional, apoptotic, and necrotic CCs of trout gills in terms of volume density as a percentage of total cell volume (A) and surface area : volume ratio (B). All data are expressed as the mean ± 1 SEM. An asterisk (*) indicates a statistically significant difference from functional CCs.

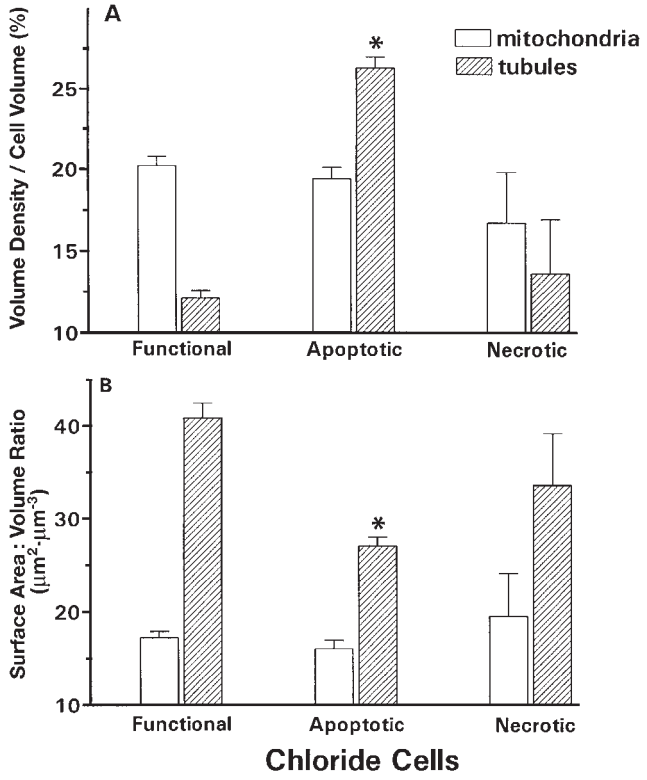

Fig. 4. Percentages of functional (hatched bars), apoptotic (open bars), and necrotic (solid bars) CCs among the total CC population measured (N = 61–87 total measurements) in 6–7 rainbow trout exposed to either pH 8.0 (control) or 9.5. An asterisk (*) or a dagger (†) indicates a statistically significant difference from control values for functional or apoptotic cells, respectively. For clarity, error bars are not included.

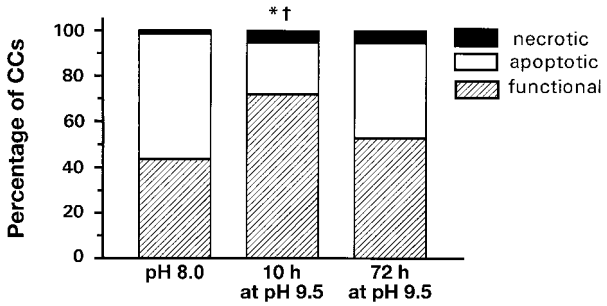

accompanied by an initial 80% reduction in the ammonia-excretion rate (J_{Amm}), which gradually recovered and approached control levels after 24 h at pH 9.5 (Table 1). The inhibition of J_{Amm} was accompanied by a simultaneous increase in plasma total ammonia concentration, which peaked at 578 μmol·L^{-1} after 24 h but then dropped by about 50% after 72 h at pH 9.5 (Table 1).

Table 2. Changes in the kinetic parameters of unidirectional chloride (Cl^-) and sodium (Na^+) uptake during exposure of rainbow trout to pH 9.5 for 72 h.

		Chloride		Sodium	
pH	Time (h)	J_{max} ($\mu mol \cdot kg^{-1} \cdot h^{-1}$)	K_m ($\mu mol \cdot L^{-1}$)	J_{max} ($\mu mol \cdot kg^{-1} \cdot h^{-1}$)	K_m ($\mu mol \cdot L^{-1}$)
8.0	C	358.2±39.9	311.0±84.8	481.5±53.1	88.5±13.3
9.5	10	172.6±30.2*	405.6±116.3	155.5±14.9*	66.2±19.8
	24	285.8±31.9	391.9±51.7	259.2±33.2*	188.3±49.0
	72	297.3±37.8	335.6±58.1	322.6±13.5*	375.2±85.4*

Note: Data are from Wilkie et al. (1999). Values are given as the mean ± 1 SEM (N = 6–7). "C" denotes control (pH 8.0) conditions.

*Significantly different from control (pH 8.0) values ($P < 0.05$).

PVCs on the filamental and lamellar surfaces were considerably different from one another in general morphology. The surfaces of the filamental PVCs were ornamented with long ridges, whereas lamellar PVCs were pleomorphic (variable morphology). The analysis of PVC surface morphometry that we employed was applied to the lamellar epithelium only, which constitutes by far the larger fraction of total PVC surface area. This approach quantifies the observed surface morphology relative to an arbitrary reference value of 100 μm^2, which represents a completely smooth surface. The PVC surface area of the lamellar epithelium under control conditions (pH 8.0) was 147 μm^2, representing a 47% increase above that of a flat surface (100 μm^2; Fig. 5B). The increase (77%) was slightly greater after 10 h, and significantly greater (143%) after 72 h at pH 9.5 (Fig. 5B; compare Fig. 9A with Fig. 9B).

Fig. 5. Changes in gill lamellar thickness (arithmetic mean) as an index of the diffusion pathway length (A) and the lamellar pavement cell (PVC) surface area in rainbow trout subjected to pH 8.0 (control; hatched bars) or pH 9.5 (open bars) for 10 or 72 h (B). Estimates of PVC surface area take into account topographical relief due to microvilli and ridges by using an arbitrary reference surface area of 100 μm^2 (10 × 10 μm), which represents a completely smooth surface. See the text for further details. All data expressed as the mean ± 1 SEM (N = 6–7 fish). An asterisk (*) indicates a statistically significant difference from control values.

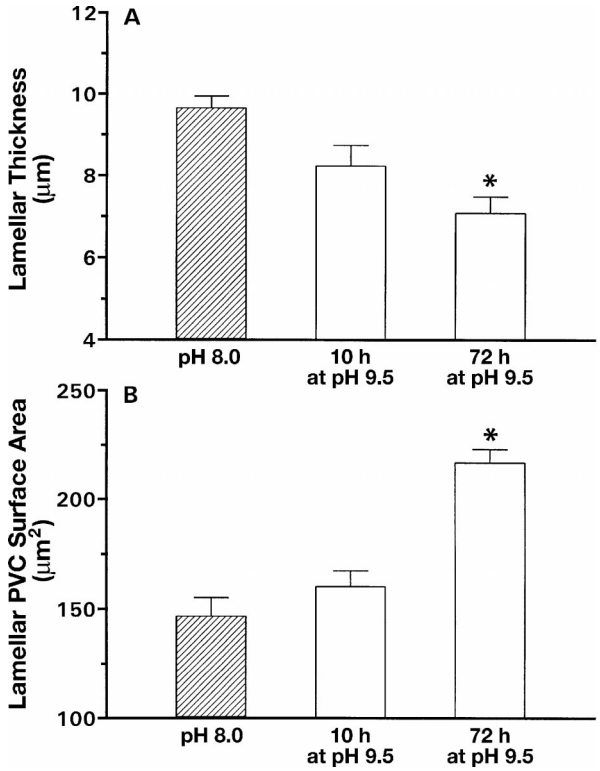

Discussion

CC morphometry and ion exchange

Recent morphological and physiological studies indicate that CCs are the sole sites of Cl^- uptake in freshwater teleosts (see reviews by Laurent and Perry 1995; Perry 1997). In some studies, significant correlations have been established between fractional surface area of CCs and both J_{in}^{Na} and J_{in}^{Cl} (e.g., Perry et al. 1992). By manipulating the acid–base status of the fish, however, it has been possible to dissociate Cl^- and Na^+ fluxes, thereby demonstrating that Cl^- uptake tracks the fractional surface area of CCs, whereas Na^+ uptake does not (Goss et al. 1994*a*, 1994*b*).

Kinetic analysis of unidirectional influx rates across the gills, measured by means of radioisotopes, demonstrated that the initial inhibition of J_{in}^{Cl} during exposure to pH 9.5 was not due to competitive inhibition by the higher concentration of OH^- ions in the water, because the K_m^{Cl} of the transporters for Cl^- did not increase (Table 2; Wilkie et al. 1999). Rather there was a reduction of the maximum transport capacity of the system for Cl^-, reflected in a significant decrease in J_{max}^{Cl}. According to two-substrate kinetic theory (Goss and Wood 1991), such a reduction in J_{max}^{Cl} can occur either because of a reduction of internal substrate availability (HCO_3^-) for exchange with Cl^- and (or) because of a real decrease in the number of functional Cl^- transport sites. Wilkie et al.'s (1999) analysis demonstrated that the reduction of J_{max}^{Cl} at 10 h was mainly due to a loss of internal HCO_3^- caused by respiratory alkalosis and simultaneous metabolic acidosis at high environmental pH, together with a small decrease in the number of functional Cl^- transport sites. Subsequent recovery was due to a real increase in the number of functional Cl^- transport sites in the face of persistent decreases in internal HCO_3^-. Concomitant with this recovery, the present study has demonstrated that the fractional surface area of CCs increased 2-fold between 10 and 72 h at high pH (Fig. 1A) as a result of an increase in the numerical density of CCs (Fig. 1B) and in the apical surface area of individual CCs (Fig. 1C). These results are in accord with the conclu-

Fig. 6. Representative scanning electron micrograph of filamental epithelium of a rainbow trout at pH 8.0 (A) or pH 9.5 (B) for 72 h. In A, note the presence of many large highly villous CCs (1), the low density of smooth CCs (2), and the low degree of PVC surface ornamentation (white asterisk). In B, note the large, smooth apical surfaces of many CCs (2) and the young, smaller, but highly villous CCs (1). In addition, the PVC surface (black asterisk) has a greater degree of ornamentation at pH 9.5. Scale bar = 10 μm.

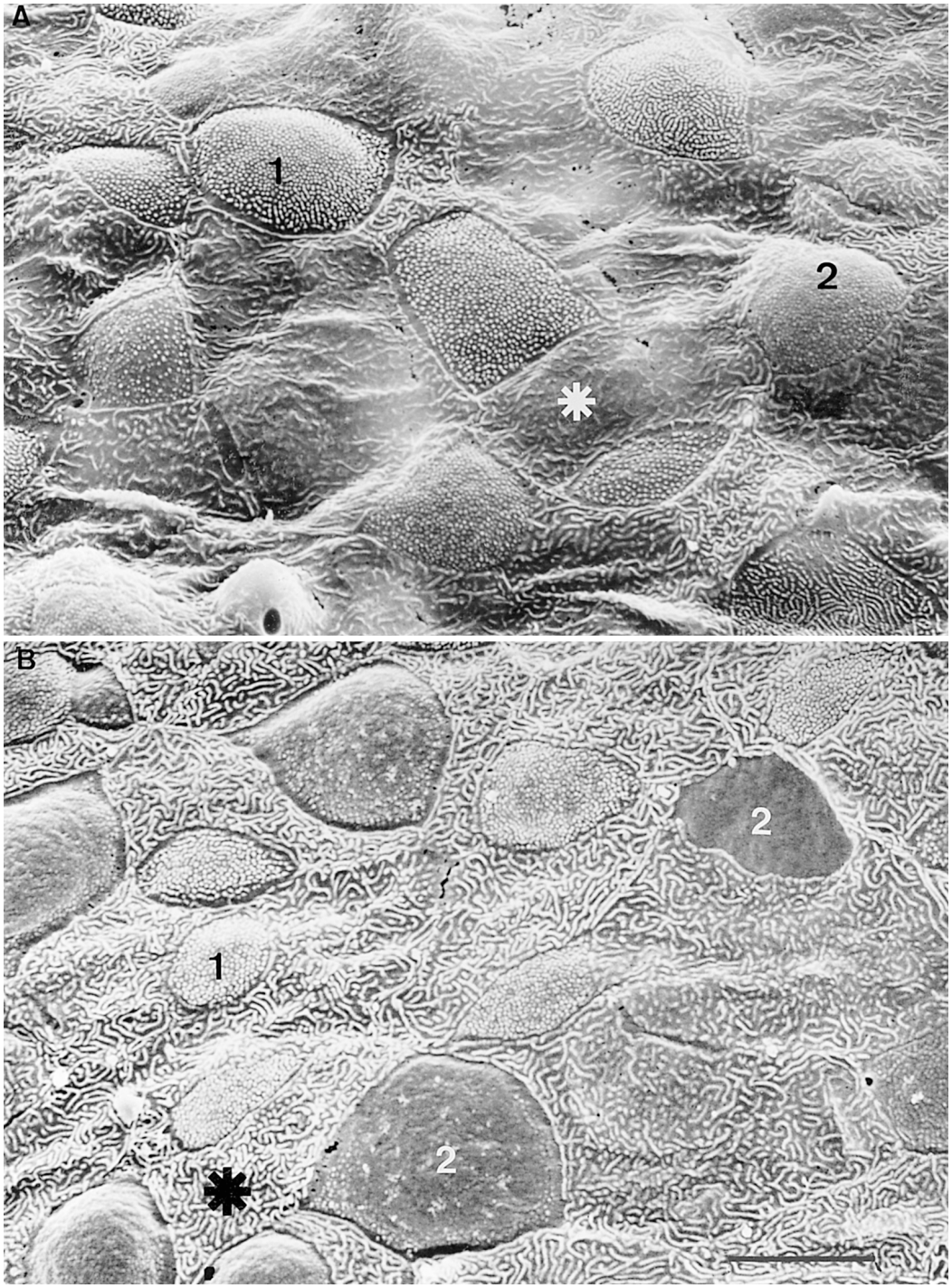

sion drawn by Wilkie et al. (1999), from two-substrate analysis, that there was a real increase in the number of Cl^- transport sites over this period. These results also support previous observations of increases in the fractional surface area of CCs in rainbow trout and Lahontan cutthroat trout (*Oncorhynchus clarki henshawi*) following transfer to pH 9.5 and to alkaline (pH 9.4) Pyramid Lake in Nevada, respectively (Wilkie and Wood 1994; Wilkie et al. 1994).

Collectively, these studies on the responses of salmonids to alkaline water suggest that CC populations are very labile, a phenomenon already reported in relation to other environmental circumstances (Laurent and Dunel 1980; Pisam et al. 1987; Laurent et al. 1994; see also the reviews of Jürss and Bastrop 1995 and Perry 1997). One problem encountered in the present study was that normal, functional CCs coexisted with a large population of apoptotic and, to a lesser extent,

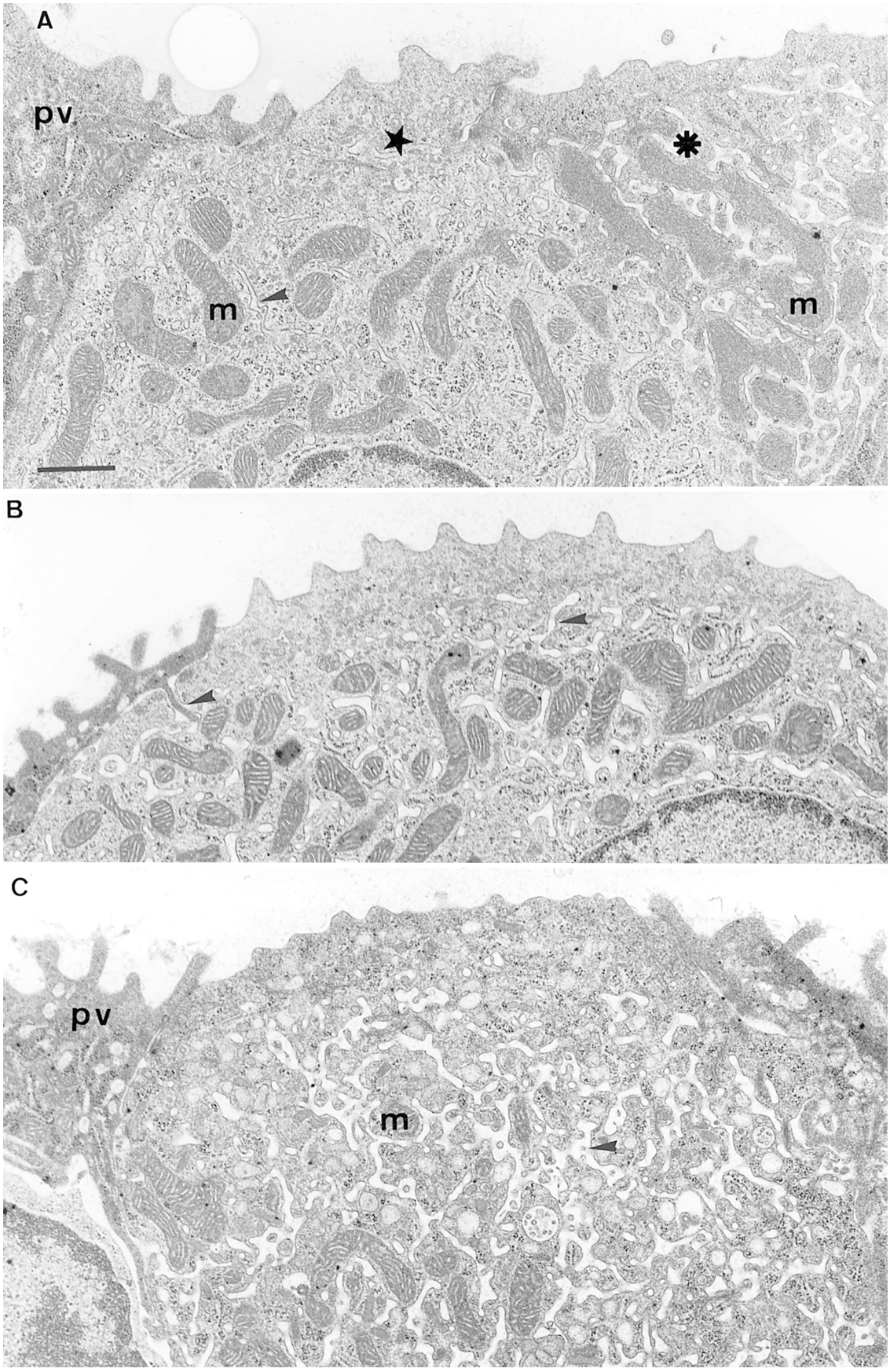

Fig. 7. Transmission electron micrographs of representative CCs. (A) A young mature chloride cell (★) beside an apoptotic CC (*). Note the small apical surface area of the young cell and the incomplete development of its tubules (arrowhead). Conversely, note the swollen tubules of the apoptotic cell and the densification of mitochondria (*m*). (B) A fully mature CC, showing an abundance of tubules clearly open to the basolateral extracellular space and well-developed apical villi. (C) In apoptotic CCs the mitochondria are unevenly distributed within the cytoplasm, and the tubules form a swollen, sinus-like compartment. The apical surface also lacks villi. *pv*, pavement cell. Scale bar = 1 μm.

Fig. 8. Representative transmission electron micrograph of gill filamental epithelium from rainbow trout 10 h after transfer from pH 8.0 to pH 9.5. Note the difference between a necrotic cell sloughing off from the epithelium surface (★) and the apoptotic cell (*). In addition, note that fully mature CCs (1) are in contact with, or positioned very near to, the external medium, while immature CCs (2) are found deeper within the epithelium. *pv*, pavement cell. Scale bar = 2 μm.

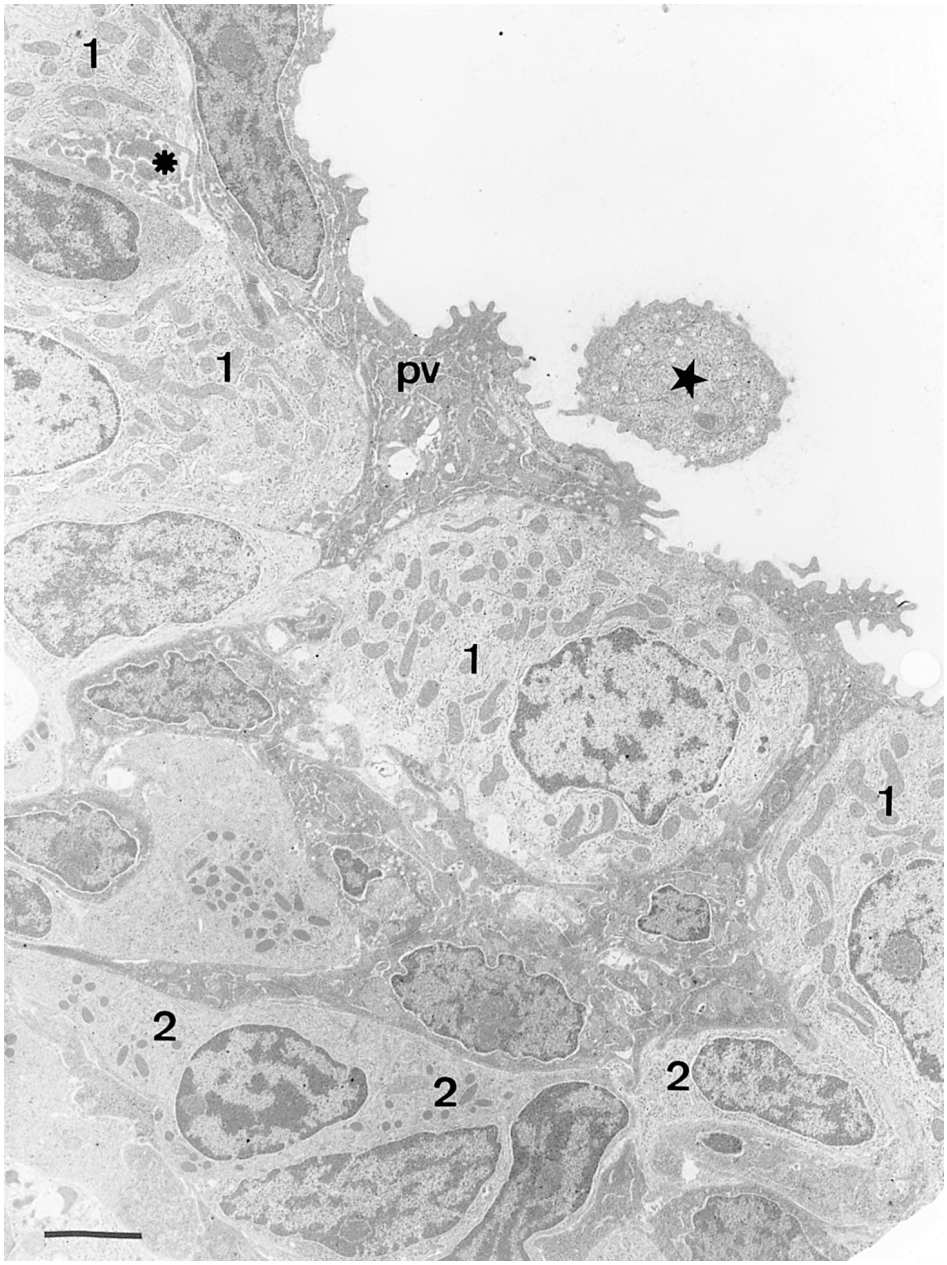

necrotic CCs. Thus, it was necessary to base our analyses on the three major stages of the CC life cycle. Using criteria first established by Wendelaar Bonga and van der Meij (1989), CCs were identified as functional (mature and immature), apoptotic (i.e., undergoing programmed cell death), or necrotic (exhibiting pronounced lysis).

Mature CCs have a well-known, thoroughly documented structure characterized by a dense, highly branched network

Fig. 9. Representative transmission electron micrograph of lamellar epithelium from rainbow trout exposed to pH 8.0 (A) and pH 9.5 (B) for 72 h. Note the presence of long microvilli on the PVC (*pv*) and the abundance of organelles in the PVC at pH 9.5. Scale bar = 1 μm.

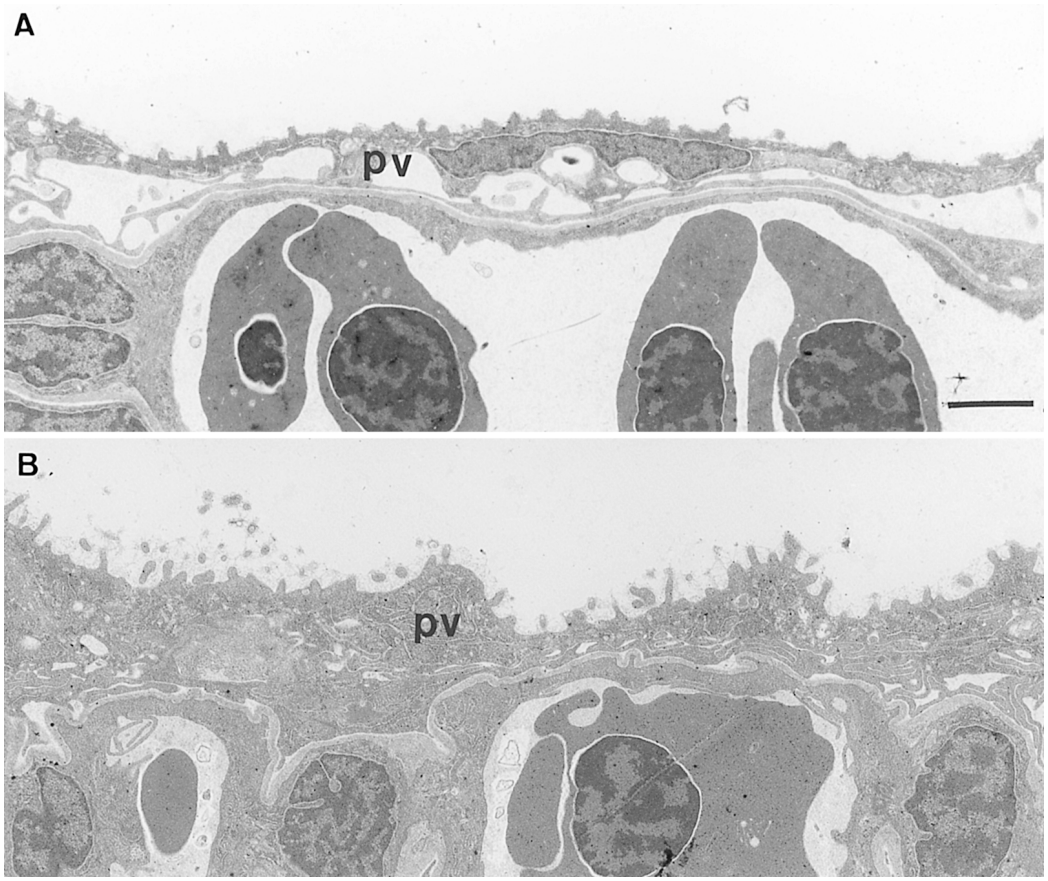

of fine intracellular tubules (for review see Laurent 1984), which are invaginations of the cell's basolateral membrane (Fig. 7B). Mature CCs also have a highly villous apical surface (Fig. 7B), but immature ("young") CCs are characterized by fewer microvilli and are therefore categorized as moderately villous (Fig. 7A). Apoptotic CCs show shrinkage and densification of the cytoplasm and nuclei, as well as a swollen tubular system (Figs. 7A, 7C). Necrotic cells are characterized by vacuolization of the cytoplasm, lysis of mitochondria, and disorganization of the tubular system, which becomes thick and interrupted. Later, necrotic cells often desquamate from the gill surface (Fig. 8). Structural differences between apoptotic and necrotic cells are related to the factors that cause cell death; apoptosis is controlled by intrinsic factors (e.g., hormonal signals), while cell death, which leads to necrosis, is caused by extrinsic factors (e.g., xenobiotics).

Compared with functional CCs, the intracellular tubules of apoptotic cells exhibited marked swelling (Fig. 3A) and a corresponding decrease in the surface area : volume ratio (i.e., tubular membrane surface area; Fig. 3B). In necrotic CCs, the volume density of tubules (Fig. 3A) and their surface area : volume ratio were intermediate between those of "functional" and apoptotic cells but highly variable. Indeed, tubules were often broken into pieces and were very thin in some places and more or less swollen in others. In contrast to the tubules, mitochondrial volume and membrane surface area : volume ratio (or external mitochondrial membrane density) were negligibly affected when functional cells became apoptotic, unless complete disorganization took place within the CC's intracellular space (Fig. 3).

In the rainbow trout gill, the apical membranes lose microvilli and become flat and smooth during apoptosis (P. Laurent, unpublished data). Indeed, this is borne out by the present results, which suggest that CCs in the initial stages of apoptosis exhibit poor ornamentation of apical surface microvilli, and this could lead to their erroneous classification as moderately villous. CCs are overlaid by PVCs during apoptosis, however, which would isolate them from the ambient water, before they are engulfed by scavenger cells (macrophages). Thus, in the present study we considered apoptotic cells to be no longer functioning, although we recognize that prior to their being covered by PVCs, their transport function could have declined progressively, though this has not yet been examined.

Apoptosis in fish gills, as in other epithelia that are subject to rapid turnover, is functionally crucial. Indeed, apoptosis was frequent in the present control fish, as more than 50% of the CCs examined exhibited internal features consistent with this process (Fig. 4). Although these values may seem high at first glance, it should be pointed out that apoptosis is common in fish gills (Wendelaar Bonga and van der Meij 1989), although the proportion of apoptotic cells in tilapia (*Oreochromis mossambicus*) was about 50% lower

than values reported here (Wendelaar Bonga et al. 1990). We have no explanation for these differences, but it is possible that environmental factors and (or) interspecific differences lead to varying rates of CC apoptosis. Indeed, proportions of apoptotic CCs have been reported to approach 50% when fish are subjected to low pH (Wendelaar Bonga et al. 1990) or changes in environmental NaCl or Ca^{2+} concentrations (Laurent 1989).

The comparative assessment of CC functional status adopted in this study, established using the above CC intracellular parameters, revealed that the percentage of apoptotic cells decreased significantly during the first 10 h following transfer to pH 9.5, before rebounding towards control levels after 72 h (Fig. 4). The lower volume density and higher surface area : volume ratio of the tubules in the total CC population observed during the first 10 h at pH 9.5 support this interpretation (Fig. 2). Collectively, these observations suggests that apoptotic degeneration is down-regulated when there is a need to restore or increase the CC population under high-pH conditions.

Using the same criteria, the above analysis also revealed that the percentage of CCs in the functional category rose within the first 10 h at pH 9.5 (Fig. 4). By 72 h, however, the proportion of functional CCs had returned almost to the control level (pH 8.0; Fig. 4). Overall, the greater proportion of functional CCs, together with fewer apoptotic cells, suggests that the rate of CC differentiation (cell turnover) is accelerated during the early stages of exposure to high pH and that programmed cell death is slowed down. This response would be beneficial because it would tend to prevent larger reductions in J_{max}^{Cl} than were observed by Wilkie et al. (1999), which might have been due to the limitations of internal substrate (HCO_3^-) supply and (or) reduced transporter numbers.

The density of micovilli in CCs was also assessed in parallel with the high pH exposure regime. Under control conditions the majority of CCs were highly villous and only a few moderately villous. If we compare these data to those presented in Fig. 4, it appears that some of the moderately villous cells, and perhaps some highly villous ones, should already be undergoing apoptosis. However, we must keep in mind that Fig. 1 is based on SEM, whereas Fig. 4 is based on TEM. Since SEM only revealed cells opened to the water, and apoptotic cells are ultimately overlaid by PVCs (Wendelaar Bonga and van der Meij 1989), we conclude that slightly more than 40% of the CCs counted using TEM were functional cells that were mainly highly villous, with some moderately villous (Figs. 1, 4).

At high pH, highly villous CCs decreased in terms of numerical density, individual apical surface area, and fractional apical surface area between 0 and 10 h (Figs. 1, 6A, 6B). The simultaneous increase in moderately villous and smooth-surfaced cells after 72 h at pH 9.5, however, is also indicative of an augmented CC turnover rate. From our TEM examinations, it was obvious that moderately villous cells were young, healthy CCs. It is well known, particularly from studies on kidney cells (for review see Brown and Breton 1996), that apical microvilli are an important characteristic of active transport cells. These data suggest that an initial decrease in the density and surface area of apical microvilli on CCs may have contributed to the decrease in J_{in}^{Cl} after the onset of exposure to alkaline conditions. Furthermore, progressive increases in the proportion of the moderately villous CC population between 10 and 72 h may have contributed to the recovery of J_{in}^{Cl}.

PVC morphology and ion exchange

Most PVCs displayed a complex structure, as previously reported (Laurent 1984; Goss et al. 1992). This study confirmed the different morphology of filamental and lamellar PVCs in *O. mykiss*, where the filamental cell surfaces are ornamented with long ridges, and lamellar PVCs are pleomorphic. The density and length of microvilli ornamenting the lamellar cells might be related to environmental conditions or PVC functional status. Although the mechanism(s) and site(s) of Na^+ uptake remain far more controversial than those of Cl^- uptake in gills of freshwater fish, recent morphological and physiological findings have favoured the so-called Na^+ channel / proton pump transport system (Avella and Bornancin 1989; Lin et al. 1994), the primary location of this system being the PVCs rather than the CCs (Goss et al. 1992, 1994*b*, 1995; Laurent et al. 1994; Sullivan et al. 1995). This evidence prompted our examination of changes in PVC morphology in relation to Na^+ uptake during exposure to high pH.

Kinetic analysis indicated a complex origin for the observed depression of J_{in}^{Na} (Wilkie et al. 1999; Table 2). Initially, a sharply decreased J_{max}^{Na} played the primary role in this reduction, but thereafter J_{max}^{Na} progressively regained control levels. These changes were largely due to real changes in the number of active Na^+ transport sites, with only a small contribution from reduced internal substrate (H^+) availability. However, at the same time, K_m^{Na} progressively increased (Table 2), and by 72 h became the predominant factor responsible for the chronic depression of J_{in}^{Na}. Wilkie et al. (1999) explained the latter as an attempt by the fish to retain H^+ in the face of chronic respiratory alkalosis. The present morphological results indicate a definite change in PVC morphometry that accompanied the simultaneous increase in both K_m^{Na} and the restoration of active Na^+ transport site numbers. In the present study, the determination of PVC surface area indicated that the density of microvilli increased progressively after the onset of exposure to high pH (Fig. 5B; compare Fig. 6A with Fig. 6B).

From TEM studies, it is well established that PVCs are active sites of membrane synthesis (Laurent et al. 1994). Clathrin-type vesicles containing putative H^+-pumps emanate from the Golgi body, and many of these appear to fuse with the plasma membrane, thereby inserting the transport proteins (for review see Perry 1997). The 143% increase in PVC surface area after 72 h at high pH indicates that similar processes took place during the present study (Fig. 5B; compare Fig. 9A with Fig. 9B). We further suggest that such a process might account for the increase in K_m^{Na} and (or) the restoration of the number of functional Na^+ transport sites during exposure to high pH. For example, the increased PVC surface area could accommodate the insertion of new Na^+ channels with lower Na^+ affinity and (or) more Na^+ channels and H^+ pumps to increase transport capacity. Indeed, the present results are generally in accord with the findings of Goss et al. (1994*b*), who observed similar changes in the PVCs of brown bullheads (*Ictalurus nebulosus*) during activation of Na^+ transport.

Ammonia excretion and diffusion distance

Another important aspect of the responses of teleosts to highly alkaline environments concerns the inhibition of branchial ammonia excretion (Wright and Wood 1985; Wilkie and Wood 1991, 1995). In the present study, the 4- to 7-fold increases in total plasma ammonia at pH 9.5 were due to the marked (80%) decrease in J_{Amm} (Table 1). The progressive recovery of J_{Amm}, which exceeded control values after 48 h, was partly due to an increase in the blood-to-water partial pressure gradient favouring outward NH_3 diffusion (Wilkie and Wood 1991; Yesaki and Iwama 1992; Wright et al. 1993). Another factor revealed by the present study was the rapid decrease in the blood-to-water diffusion distance (Fig. 5A), which was significant after 72 h. It is doubtful that such an effect would have been large enough by itself (a 27% decrease) to account for the complete recovery of J_{Amm} reported by Wilkie et al. (1999), but previous studies clearly demonstrated an association between gas-exchange (O_2, CO_2) efficiency and the length of the diffusion pathway across trout gills (Bindon et al. 1994; Greco et al. 1995).

Acknowledgements

This study was supported by a Natural Sciences and Engineering Research Council of Canada (NSERC) research grant to C.M.W. and an NSERC Foreign Researcher Award to P.L. P.L. also held a Hooker Distinguished Professor Visiting Fellowship at McMaster University, where part of this paper was written. M.P.W. was supported by an Ontario Graduate Scholarship.

References

Avella M., and Bornancin, M. 1989. A new analysis of ammonia and sodium transport through the gills of the freshwater rainbow trout (*Salmo gairdneri*). J. Exp. Biol. **142**: 155–175.

Bindon, S.D., Gilmour, K.M., Fenwick, J.C., and Perry, S.F. 1994. The effects of branchial chloride cell proliferation on respiratory function in the rainbow trout *Oncorhynchus mykiss*. J. Exp. Biol. **197**: 47–65.

Brett J.R., and Zala, C.A. 1975. Daily pattern of nitrogen excretion and oxygen consumption of sockeye salmon (*Oncorhynchus kisutch*) under controlled conditions. J. Fish. Res. Board Can. **32**: 2479–2486.

Brown, D., and Breton, S. 1996. Mitochondria-rich proton-secreting epithelial cells. J. Exp. Biol. **199**: 2345–2358.

Coleman, M.E., and Johnson, V.K. 1988. Summary of management at Pyramid Lake, Nevada, with emphasis on Lahontan cutthroat trout. Am. Fish. Soc. Symp. No. 4. pp. 107–115.

Goss, G.G., and Wood, C.M. 1991. Two-substrate kinetic analysis: a novel approach linking ion and acid–base transport at the gills of freshwater trout, *Oncorhynchus mykiss*. J. Comp. Physiol. B, **161**: 635–646.

Goss, G.G., Perry, S.F, Wood, C.M., and Laurent, P. 1992. Mechanisms of ion and acid–base regulation at the gills of freshwater fish. J. Exp. Zool. **263:** 143–159.

Goss, G.G., Laurent P., and Perry, S.F. 1994*a*. Gill morphology during hypercapnia in brown bullhead (*Ictalurus nebulosus*): role of chloride cells and pavement cells in acid–base regulation. J. Fish Biol. **45**: 705–718.

Goss, G.G., Wood, C.M., Laurent P., and Perry, S.F. 1994*b*. Morphological responses of the rainbow trout (*Oncorhynchus mykiss*) gill to hyperoxia, base ($NaHCO_3$) and acid (HCl) infusions. Fish Physiol. Biochem. **12**: 465–477.

Goss, G.G., Perry, S., and Laurent, P. 1995. Ultrastructural and morphometric studies on ion and acid–base transport processes in freshwater fish. *In* Fish physiology. Vol. 14. Cellular and molecular approaches to fish ionic regulation. *Edited by* C.M. Wood and T.J. Shuttleworth. Academic Press, New York. pp. 257–284.

Greco, A.M., Gilmour, K.M., Fenwick, J.C., and Perry, S.F. 1995. The effects of soft water acclimation on respiratory transfer in the rainbow trout *Oncorhynchus mykiss*. J. Exp. Biol. **198**: 2557–2567.

Halstead, B.G., and Tash, J.C. 1982. Unusual diel pHs in water as related to aquatic vegetation. Hydrobiologia, **96**: 217–224.

Heming T.A., and Blumhagen, K.A. 1988. Plasma acid–base and electrolyte status of rainbow trout exposed to alum (aluminum sulphate) in acidic and alkaline environments. Aquat. Toxicol. **12**: 125–140.

Jürss, K., and Bastrop, R. 1995. The function of mitochondria-rich cells (chloride cells) in teleost gills. Rev. Fish Biol. Fish. **5**: 235–255.

Kucera P.A., Koch, D.L., and Marco, G.F. 1985. Introductions of Lahontan cutthroat trout into Omak Lake, Washington. N. Am. J. Fish. Manage. **5**: 296–301.

Laurent, P. 1984. Gill internal morphology. *In* Fish physiology. Vol. 10A. *Edited by.* W.S. Hoar and D.J. Randall. Academic Press, New York. pp. 73–183.

Laurent, P. 1989. Gill structure and function: fish. *In* Comparative pulmonary physiology. *Edited by* Stephen C. Wood. Marcel Dekker Publisher, New York and Basel. pp. 69–120.

Laurent, P., and Dunel, S. 1980. Morphology of gill epithelia in fish. Am. J. Physiol. **238**: R147–R159.

Laurent, P., and Hebibi, N. 1989. Gill morphometry and fish osmoregulation. Can. J. Zool. **67**: 3055–3063.

Laurent, P., and Perry, S.F. 1990. Effects of cortisol on gill chloride cell morphology and ionic uptake in freshwater trout, *Salmo gairdneri*. Cell Tissue Res. **259**: 429–442.

Laurent, P., and Perry, S.F. 1995. Morphological basis of acid–base and ion regulation in fish. *In* Advances in comparative and environmental physiology. Mechanisms of systemic regulation: acid–base regulation, ion transfer and metabolism. *Edited by* N. Heisler. Springer-Verlag, Heidelberg. pp. 91–118.

Laurent, P., Goss, G.G., and Perry, S.F. 1994. Proton pumps in fish gill pavement cells? Arch. Int. Physiol. Biochim. Biophys. **102**: 77–79.

Lin, H., Pfeiffer, D.C., Vogl, A.W., Pan, J., and Randall, D.J. 1994. Immunolocalization of proton-ATPase in the gill epithelia of rainbow trout. J. Exp. Biol. **195**: 169–183.

Merz, W.A. 1968. Streckenmessung an gerichteten Strukturen im Mikroskop und ihre Anwendung zur Bestimung von Oberflächen-Volumen-Relationen in Knochengewebe. Mikroskopie, **22**: 132–144.

Murray, C.A., and Zeibell, C.D. 1984. Acclimation of rainbow trout to high pH to prevent stocking mortality in summer. Prog. Fish-Cult. **46**: 176–179.

Perry, S.F. 1997. The chloride cell: structure and function in the gills of freshwater fishes. Annu. Rev. Physiol. **59**: 325–47.

Perry, S.F., and Laurent, P. 1989. Adaptational responses of rainbow trout to lowered external NaCl concentration: contribution of the branchial chloride cell. J. Exp. Biol. **147**: 147–168.

Perry, S.F., Goss, G.G., and Laurent, P. 1992. The interrelationships between gill chloride cell morphology and ionic uptake in four freshwater teleosts. Can. J. Zool. **70**: 1775–1786.

Pisam, M., Caroff, A., and Rambourg, A. 1987. Two types of chloride cells in the gill epithelium of a freshwater-adapted

euryhaline fish *Lebistes reticulatus*; their modifications during adaptation to saltwater. Am. J. Anat. **179**: 40–50.

Sullivan, G.V., Fryer, J.N., and Perry, S.F. 1995. Immunolocalization of proton pumps (H^+-ATPase) in pavement cells of rainbow trout gill. J. Exp. Biol. **198**: 2619–2629.

Wagner, E.J., Bosakowski, T., and Intelmann, S. 1997. Combined effects of temperature and high pH on mortality and the stress response of rainbow trout after stocking. Trans. Am. Fish. Soc. **126**: 985–998.

Weibel, E.R., and Bolender, R.P. 1973. Stereological techniques for electron microscopic morphometry. *In* Principles and techniques of electron microscopy. Vol. 3. *Edited by* M.A. Hayat. Van Nostrand Reinhold Co., New York. pp 237–296.

Weibel, E.R., and Knight, B.W. 1964. A morphometric study on the thickness of the pulmonary air–blood barrier. J. Cell Biol. **21**: 367–384.

Weibel, E.R., Kistler, G.S., and Scherle, W.P. 1966. Practical stereological methods for morphometric cytology. J. Cell Biol. **30**: 23–38.

Wendelaar Bonga, S.E., and van der Meij, C.J.M. 1989. Degeneration and death, by apoptosis and necrosis, of the pavement and chloride cells in the gills of the teleost *Oreochromis mossambicus*. Cell Tissue Res. **255**: 235–243.

Wendelaar Bonga, S.E., Flik, G., Balm, P.H.M., and van der Meij, C.J.M. 1990. The ultrastructure of chloride cells in the gills of the teleost *Oreochromis massambicus* during exposure to acidified water. Cell Tissue Res. **259**: 575–585.

Wilkie, M.P., and Wood, C.M. 1991. Nitrogenous waste excretion, acid–base regulation, and ionoregulation in rainbow trout (*Oncorhynchus mykiss*) exposed to extremely alkaline water. Physiol. Zool. **64**: 1069–1086.

Wilkie, M.P., and Wood, C.M. 1994. The effects of extremely alkaline water (pH 9.5) on rainbow trout gill function and morphology. J. Fish Biol. **45**: 87–98.

Wilkie, M.P., and Wood, C.M. 1995. Recovery from high pH exposure in the rainbow trout: white muscle ammonia storage, ammonia washout and the restoration of blood chemistry. Physiol. Zool. **68**: 379–401.

Wilkie, M.P., P.A. Wright, G.K. Iwama, and C.M. Wood. 1993. The physiological responses of the Lahontan cutthroat trout (*Oncorhynchus clarki henshawi*), a resident of highly alkaline Pyramid Lake (pH 9.4), to challenge at pH 10. J. Exp. Biol. **175**: 173–194.

Wilkie, M.P., Wright, P.A., Iwama, G.K., and Wood, C.M. 1994. The physiological adaptations of the Lahontan cutthroat trout (*Oncorhynchus clarki henshawi*), following transfer from fresh water to the highly alkaline waters of Pyramid Lake, Nevada (pH 9.4). Physiol. Zool. **67**: 355–380.

Wilkie, M.P., Simmons, H.E., and Wood, C.M. 1996. Physiological adaptations of rainbow trout to chronically elevated water pH (pH = 9.5). J. Exp. Zool. **274**: 1–14.

Wilkie, M.P., Laurent, P., and Wood, C.M. 1999. Differential regulation of Na^+ and Cl^- movements across rainbow trout gills: the influence of highly alkaline (pH = 9.5) water. Physiol. Biochem. Zool. **72**: 360–368

Wright, P.A. 1993. Nitrogen excretion and enzyme pathways for ureagenesis in freshwater tilapia (*Oreochromis niloticus*). Physiol. Zool. **66**: 881–901.

Wright, P.A., and Wood, C.M. 1985. An analysis of branchial ammonia excretion in the freshwater rainbow trout: effects of environmental pH change and sodium uptake blockade. J. Exp. Biol. **114**: 329–353.

Wright, P.A., Iwama, G.K., and Wood, C.M. 1993. Ammonia and urea excretion in Lahontan cutthroat trout (*Oncorhynchus clarki henshawi*) adapted to highly alkaline Pyramid Lake (pH 9.4). J. Exp. Biol. **175**: 153–172.

Yesaki, T.Y., and Iwama, G.K. 1992. Some effects of water hardness on survival, acid–base regulation, ion regulation and ammonia excretion in rainbow trout in highly alkaline water. Physiol. Zool. **65**: 763–787.